DOI 10.1007/s10891-018-1824-x

Journal of Engineering Physics and Thermophysics, Vol. 91, No. 4, July, 2018

FREE CONVECTIVE FLOW, HEAT AND MASS TRANSFER IN A MICROPOLAR FLUID OVER A SHRINKING SHEET IN THE PRESENCE OF A HEAT SOURCE

S. R. Mishra,[a] J. Mohanty,[b] and J. K. Das[b]

UDC 536.5

The paper considers a free convective flow of a micropolar fluid in the presence of a heat source/sink over a shrinking sheet. Similarity transformations are used to reduce the governing coupled nonlinear partial differential equations, namely, the momentum and concentration equations, as well as the nonhomogeneous heat equation, to a set of nonlinear ordinary differential equations. Their numerical solution is obtained by the Runge–Kutta fourth-order method accompanied by the shooting technique. The effects of various physical parameters characterizing the flow are studied. The validation of the present results by the earlier published ones is performed in a particular case, and good agreement is obtained.

Keywords: *micropolar fluid, free convection, shrinking sheet, heat and mass transfer, Runge–Kutta method.*

Introduction. The theory of micropolar fluids has attracted considerable attention in the last few decades due to its importance in many technological applications, such as cooling of electronic devices and nuclear reactors during emergency shutdown, enhancing oil recovery, etc. Flows over a shrinking surface are encountered in several technological processes. Such situations occur in polymer processing, manufacture of glass sheets, paper and textile production, and in numerous other fields. From the engineering point of view, boundary-layer flows of a non-Newtonian fluid over a stretching sheet are always of importance. They are widely applied in extrusion processes, wire drawing, glass fiber and paper production, movement of biological fluids, and in food processing. The heat and mass transfer analysis of boundary-layer flows with thermal radiation and chemical reaction are also important in several industrial areas. Eringen [1] developed the theory of micropolar fluids, which cannot be described by the classical Navier–Stokes equations due to the micro-inertia and spin, or the microrotational effects. A boundary-layer flow of an incompressible micropolar fluid over a semi-infinite plate was studied by Ahmadi [2] who obtained a self-similar solution of the governing partial differential equations. Gorla [3] investigated a micropolar boundary-later stagnation-point flow on a moving wall.

In the last few years, the application of fluid flows past a stretching surface has received wide attention of researchers in the field of metallurgy and chemical engineering. The pioneer work was published by Crane [4] who obtained an analytical solution for a laminar boundary-layer flow past a stretching sheet. The study of a liquid film on an unsteady stretching sheet was presented by Wang [5]. Hayat and Qasim [6] considered the effects of thermal radiation and magnetic field on an unsteady mixed-convection flow of a second-grade fluid over a vertical stretching sheet. Pal and Mondal [7] studied the influence of a nonuniform heat source/sink, variable viscosity, and the Soret effect on MHD non-Darcy mixed convective diffusion of species over a stretching sheet embedded in a porous medium. A magnetohydrodynamic flow of a power-law fluid over a stretching sheet was considered by Cortell [8]. A boundary-layer stagnation-point flow of a Casson fluid and heat transfer towards a shrinking/stretching sheet were analyzed by Bhattacharya [9]. Yacob, Ishak, and Pop [10] investigated melting heat transfer in a boundary-layer stagnation-point flow towards a stretching/shrinking sheet in a micropolar fluid.

The physical nature of flows induced by a shrinking sheet is quite different from that due to a stretching one. The works on a shrinking sheet were generalized to include a stagnation flow, which is a backward one. Miklavčič and Wang [13] studied a viscous flow due to a shrinking sheet. They obtained an exact solution of the Navier–Stokes equations and showed that mass suction is required to maintain a flow over a shrinking sheet. Mohanty, Mishra, and Pattnaik [14] presented a numerical investigation on heat and mass transfer in a micropolar fluid flow over a stretching sheet. Mishra, Dash, and

[a]Department of Mathematics, Siksha 'O' Anusandhan Deemed to be University, Bhubaneswar-751030, Odisha, India; email: satyaranjan_mshr@yahoo.co.in; [b]Department of Physics, Stewart Science College, Cuttack, India. Published in Inzhenerno-Fizicheskii Zhurnal, Vol. 91, No. 4, pp. 1043–1049, July–August, 2018. Original article submitted July 18, 2016; revision submitted March 15, 2018.

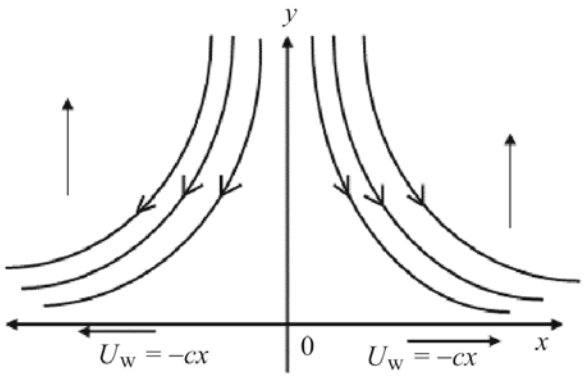

Fig. 1. Flow geometry.

Pattnaik [15] investigated heat and mass transfer on MHD free-convection in a micropolar fluid with a heat source. Rout et al. [16] studied the chemical reaction effect on an MHD free-convection flow in a micropolar fluid. A nonperturbative solution for an MHD viscous flow due to a shrinking sheet was analyzed by Noor, Kechil, and Hashim [17]. Ishak, Lok, and Pop [18] investigated a stagnation-point flow over a shrinking sheet in a micropolar fluid. They also extended their work to a non-Newtonian power-law fluid flow past a shrinking sheet with suction [19]. Several researchers [20–25] studied a non-Newtonian fluid flow past a shrinking sheet by means of different models, solving the problem both analytically and numerically. Bhattacharyya et al. [26] investigated the effect of thermal radiation on a micropolar fluid flow and heat transfer over a porous shrinking sheet.

Inspired by the above studies, we consider a steady flow of a micropolar fluid and heat transfer over a porous shrinking sheet in the presence of a heat source and chemical reaction. The numerical solution of the problem is obtained by the Runge–Kutta method accompanied by the shooting technique. The validation of the present results by those from the earlier published works is carried out.

Formulation of the Problem. A steady two-dimensional flow of a micropolar fluid with heat and mass transfer over a porous shrinking sheet is considered (see Fig. 1). The shrinking velocity of the sheet is $U_w = -cx$, where c is a shrinking constant, such that $c > 0$. The corresponding equations in the boundary-layer approximation are as follows:

$$\frac{\partial u}{\partial x} + \frac{\partial v}{\partial y} = 0 , \tag{1}$$

$$\rho \left(u \frac{\partial u}{\partial x} + v \frac{\partial u}{\partial y} \right) = (\mu + \kappa) \frac{\partial^2 u}{\partial y^2} + \kappa \frac{\partial N}{\partial y} + g\rho\beta'(T - T_\infty) + g\rho\beta^*(C - C_\infty) , \tag{2}$$

$$\rho j \left(u \frac{\partial N}{\partial x} + v \frac{\partial N}{\partial y} \right) = \gamma \frac{\partial^2 N}{\partial y^2} - \kappa \left(2N + \frac{\partial u}{\partial y} \right) , \tag{3}$$

$$\rho c_p \left(u \frac{\partial T}{\partial x} + v \frac{\partial T}{\partial y} \right) = \kappa^* \frac{\partial^2 T}{\partial y^2} - \frac{\partial q_r}{\partial y} + Q^*(T - T_\infty) , \tag{4}$$

$$u \frac{\partial C}{\partial x} + v \frac{\partial C}{\partial y} = D \frac{\partial^2 C}{\partial y^2} - Kc^*(C - C_\infty) , \tag{5}$$

and the boundary conditions are

$$\begin{gathered} u = U_w = -cx , \quad v = v_w , \quad N = -m \frac{\partial u}{\partial y} , \quad T = T_w , \quad C = C_w \quad \text{at} \quad y = 0 ; \\ u \to 0 , \quad N \to 0 , \quad T \to T_\infty , \quad C \to C_\infty \quad \text{as} \quad y \to \infty . \end{gathered} \tag{6}$$

Here T_w and T_∞ are the fluid temperature near the plate and the ambient temperature assumed to be constant; $v_w < 0$ corresponds to suction and $v_w > 0$, to injection. It should be mentioned that m is a constant called the surface condition parameter, such that $0 \le m \le 1$. The case of $m = 0$ corresponds to $N = 0$ at the surface, which presents a flow of concentrated particles where the microelements close to the wall surface are unable to rotate. This case is also known as a strong concentration of microelements. The value $m = 0.5$ corresponds to vanishing of the antisymmetric part of the stress tensor and to a weak concentration of microelements, whereas $m = 1$, to turbulent boundary-layer flows.

Following [18], we assume that the spin gradient viscosity is given by

$$\gamma = (\mu + \kappa/2) j = \mu \left(1 + \frac{\Delta}{2}\right) j ,$$

where $\Delta = \kappa/\mu$ is the material parameter. This assumption allows us to predict the correct flow behavior in the limiting case, where the microstructure effects become negligible and the total spin N reduces to the value of the angular velocity.

Using the Rosseland approximation for radiation, we obtain $q_r = -\dfrac{4\sigma}{3k}\dfrac{\partial T^4}{\partial y}$. We assume that the temperature variation within the flow is such that T^4 may be expanded into a Taylor series. After expanding and neglecting the higher-order terms, we get $T^4 = 4T_\infty^3 T - 3T_\infty^4$. Now Eq. (4) reduces to

$$u\frac{\partial T}{\partial x} + v\frac{\partial T}{\partial y} = \frac{\kappa^*}{\rho c_p}\frac{\partial^2 T}{\partial y^2} + \frac{16\sigma T_\infty^3}{3k\rho c_p}\frac{\partial^2 T}{\partial y^2} + \frac{Q^*}{\rho c_p}(T - T_\infty) . \tag{7}$$

The following stream function and similarity variables are introduced:

$$\psi = \sqrt{c\upsilon}\, x f(\eta) , \quad N = cx\sqrt{c/\upsilon}\, h(\eta) , \tag{8}$$

$$T = T_\infty + (T_w - T_\infty)\theta(\eta) , \quad C = C_\infty + (C_w - C_\infty)\phi(\eta) , \tag{9}$$

where $\eta = \sqrt{c/\upsilon}\, y$, $u = \dfrac{\partial \psi}{\partial y}$, $v = -\dfrac{\partial \psi}{\partial x}$. Now Eq. (1) is satisfied identically, and Eqs. (2), (3), (5), and (7) reduce to the following nonlinear coupled ordinary differential equations:

$$(1 + \Delta) f f''' + f f'' - f'^2 + \Delta h' + \mathrm{Gr}\ \theta + \mathrm{Gc}\ \phi = 0 , \tag{10}$$

$$(1 + \Delta/2) h'' + f h' - f' h - \Delta(2h + f'') = 0 , \tag{11}$$

$$(3R + 4)\theta'' + 3R\ \mathrm{Pr}\ f\theta' + 3R\ \mathrm{Pr}\ \beta\theta = 0 , \tag{12}$$

$$\frac{1}{\mathrm{Sc}}\phi'' + 3f\phi' - Kc\phi = 0 , \tag{13}$$

where the primes denote differentiation with respect to η, $\mathrm{Pr} = \mu c_p/\kappa^*$, $R = \kappa^* k/4\sigma T_\infty^3$, $\mathrm{Sc} = \upsilon/D$, $\mathrm{Gr} = \dfrac{\upsilon g \beta'(T_w - T_\infty)}{c^2 x}$, $\mathrm{Gc} = \dfrac{\upsilon g \beta^*(C_w - C_\infty)}{c^2 x}$, $\beta = \dfrac{Q^*}{c\rho c_p}$, and $Kc = \dfrac{Kc^*}{c}$.

The transformed boundary conditions are

$$f(\eta) = S , \quad f'(\eta) = -1 , \quad h(\eta) = -mf''(\eta) , \quad \theta(\eta) = 1 , \quad \phi(\eta) = 1 \quad \text{at} \quad \eta = 0 , \tag{14}$$

$$f'(\eta) \to 0 , \quad h(\eta) \to 0 , \quad \theta(\eta) \to 0 , \quad \phi(\eta) \to 0 \quad \text{as} \quad \eta \to \infty , \tag{15}$$

where $S = -v_w/(c\upsilon)^{1/2}$ is the wall mass transfer parameter with $S > 0$ corresponding to mass suction and $S < 0$, to mass injection.

Numerical Method. The set of nonlinear coupled differential equations (10)–(13) subject to boundary conditions (14) and (15) constitutes a two-point boundary-value problem. In order to solve these equations numerically, we follow the most efficient numerical shooting technique with the Runge–Kutta scheme. Following the superposition method, the ordinary differential equations (10)–(13) are formulated initially as a set of the first-order simultaneous equations with seven unknowns. Thus, we set $y_1 = f$, $y_2 = f'$, $y_3 = f''$, $y_4 = h$, $y_5 = h'$, $y_6 = \theta$, $y_7 = \theta'$, $y_8 = \phi$, and $y_9 = \phi'$. Then Eqs. (10)–(13) are reduced to a system of ordinary differential equations, namely,

$$y_3' = (-y_1 y_3 + y_2^2 - \Delta y_5 - \mathrm{Gr} y_6 - \mathrm{Gc} y_8)/(1 + \Delta) y_1 ,$$

$$y_5' = -y_1 y_5 + y_2 y_4 + \Delta(2y_4 + y_3) \Big/ \left(1 + \frac{\Delta}{2}\right),$$

$$y_7' = \frac{-R\ \mathrm{Pr}}{4 + 3R} (3y_1 y_7 + 3\beta y_6) ,$$

$$y_9' = -\mathrm{Sc}(3y_1 y_9 - Kc\, y_8)$$

with the boundary conditions

$$y_1(0) = S , \quad y_2(0) = -1 , \quad y_2(\infty) = 0 , \quad y_4(0) = -m y_3(0) ,$$
$$y_4(\infty) = 0 , \quad y_6(0) = 1 , \quad y_6(\infty) = 0 , \quad y_8(0) = 1 , \quad y_8(\infty) = 0 .$$

The solution process is repeated with large values of η_∞ until two successive values of $f''(0)$, $h''(0)$, $\theta'(0)$, and $\phi'(0)$ differ only in a desired decimal digit. The last value of η_∞ is chosen as an appropriate value corresponding to the limit $\eta \to \infty$ for that particular set of parameters. The procedure is repeated until we get the results up to a desired range of accuracy, namely, 10^{-6}.

Results and Discussion. A free-convection flow of an incompressible micropolar fluid over a porous shrinking sheet in the presence of a heat source/sink and chemical reaction has been considered. The species concentration change was taken into account. The governing differential equations were solved numerically, using the Runge–Kutta fourth-order method followed by the shooting technique. For validation of the present results, we have compared them with those from [24] regarding the skin friction and mass diffusion rate at the surface, and good agreement has been shown. The results are presented in Figs. 2–8 and in Table 1. It should be mentioned that $m = 0.5$ throughout the figures.

The velocity profiles are presented in Figs. 2–5. It is seen that they begin from negative values satisfying the boundary conditions and then tend to zero asymptotically. The influence of the wall mass suction parameter S on the velocity profile is shown in Fig. 2. It is seen that the velocity magnitude decreases with increase in S. Figure 3 shows the effect of S on the velocity profile both in the case of $\mathrm{Gr} = \mathrm{Gc} = 0$, $\beta = 0$ and for $\mathrm{Gr} = 1$, $\beta = 0.1$. It is observed that in the absence of a heat source $(\beta = 0)$ the velocity magnitude increases with Gr. In the presence of both free convection and a heat source $(\mathrm{Gr} = 0.1$ and $\beta = 0.1)$, as the wall suction parameter increases, there is a slight increase in the velocity magnitude. It should be noted that our results are in good agreement with data from [24] in a particular case of $\mathrm{Gr} = 0$ and $\beta = 0$.

Figures 4 and 5 illustrate the effect of the source parameter β on the velocity with the variations in the material parameter Δ, as well as in Gr and Gc. For the verification, we compared our results with those from [24] in a particular case of $\mathrm{Gr} = 0$ and $\beta = 0$. From Fig. 4 it is interesting to note that at $\mathrm{Gr} = 1$, $\beta = 1$ and in the absence of mass transfer ($\mathrm{Gc} = 0$) the velocity magnitude decreases slightly with increase in Δ. However, an increase in the thermal buoyancy parameter Gr and in the mass solutal buoyancy parameter Gc has the opposite effect both in the presence and in the absence of a source. It is seen that an increase in the heat source parameter accelerates the flow for $\eta \le 3$ and then retards it. It is also observed that the results presented in Figs. 4 and 5 actually coincide.

The influence of the variations in S, Gr, and β on the angular velocity distribution in the absence of solutal buoyancy is shown in Fig. 6. It is observed that the angular velocity remains negative in the boundary layer. It is interesting to note that

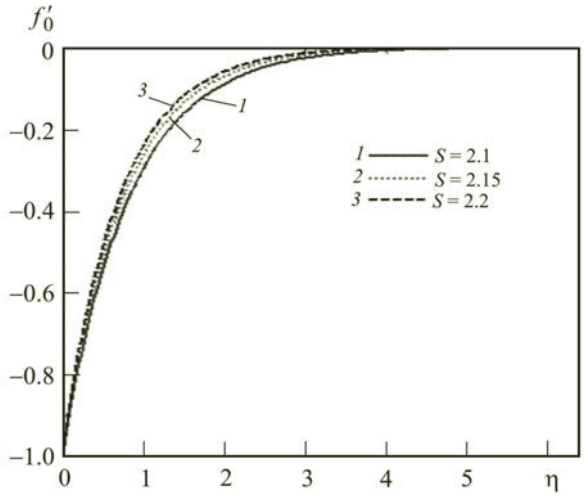

Fig. 2. Velocity profiles for Δ = 0.1, Gr = Gc = 1, and different *S*.

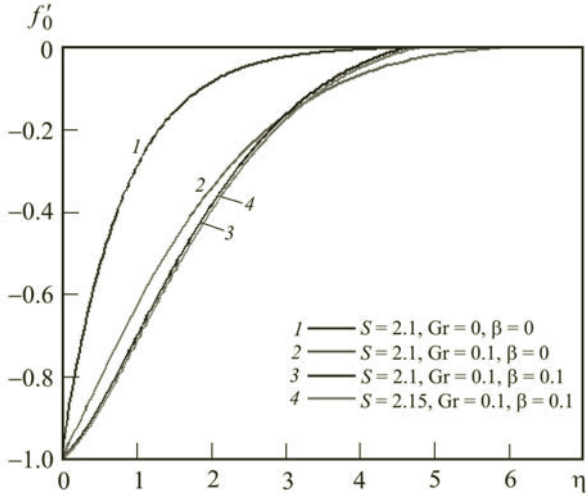

Fig. 3. Velocity profiles for Δ = 0.1, Gc = 0, and different *S*, Gr, and β.

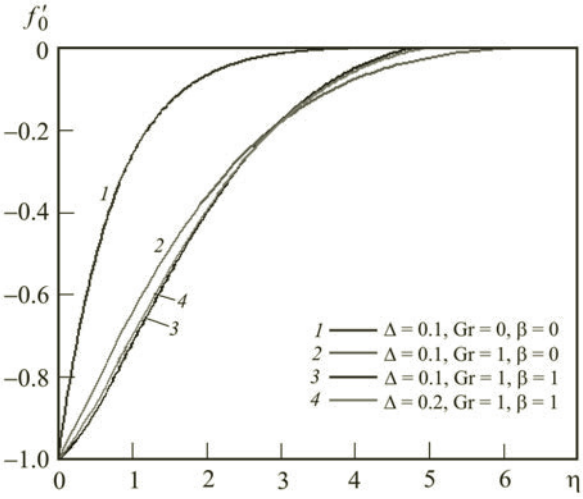

Fig. 4. Velocity profiles for *S* = 2.15, Gc = 0, and different Δ, Gr, and β.

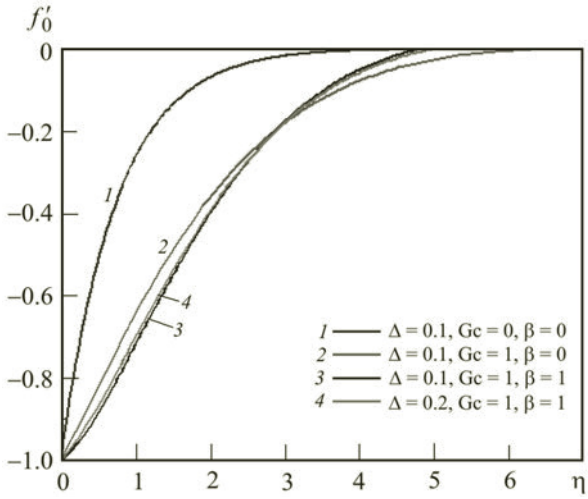

Fig. 5. Velocity profiles for *S* = 2.15, Gr = 0, and different Δ, Gc, and β.

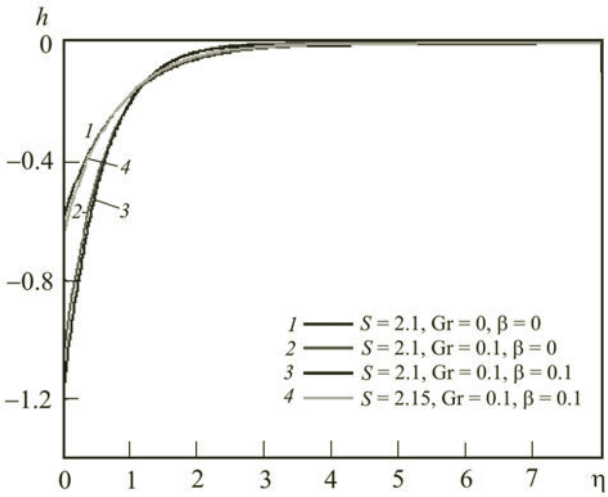

Fig. 6. Angular velocity profiles for Δ = 0.1, Gc = 0, and different *S*, Gr, and β.

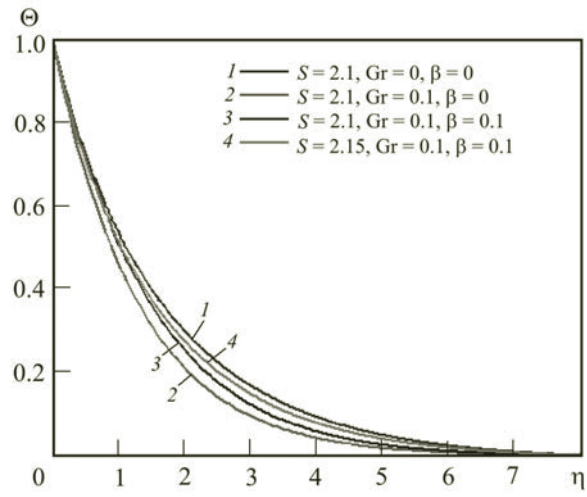

Fig. 7. Temperature profiles for Δ = 0.1, Gc = 0, and different *S*, Gr, and β.

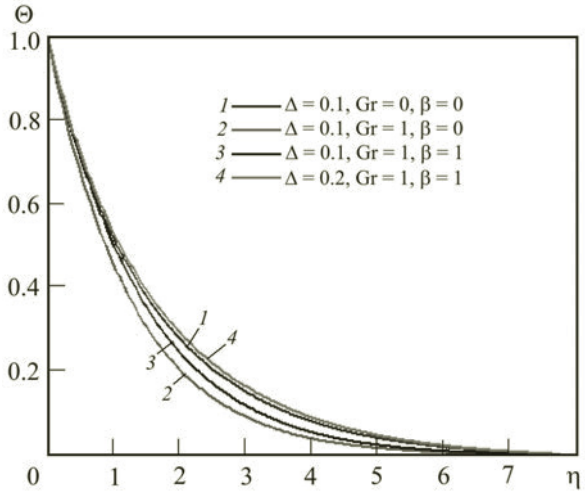

Fig. 8. Temperature profiles for $S = 2.15$, Gc = 1, and different Δ, Gr, and β.

TABLE 1. Skin Friction Coefficient, Couple Stress Coefficient, and Nusselt Number

Parameters	$f''(0)$	$h'(0)$	$-\theta'(0)$	Parameters	$f''(0)$	$h'(0)$	$-\theta'(0)$
S	Gr = Gc = 0, β = 0, $k = 0.1$, $m = 0.5$, $R = 1$			S	Gr = Gc = 0.1, β = 0.1, $k = 0.1$, $m = 0.5$, $R = 1$		
2.10	1.218612	0.742453	0.674254	2.10	0.149285	–0.44082	0.22125
2.15	1.333451	0.889024	0.712144	2.15	0.120955	–0.48226	0.232077
2.20	1.428628	1.020475	0.745672	2.20	0.09332	–0.5251	0.244206
k	Gr = Gc = 0.1, β = 1, $m = 0.5$, $S = 2.15$, $R = 1$			Gc	Gr = 0, β = 0, $K = 0.1$, $m = 0.5$, $S = 2.15$, $R = 1$		
0.1	2.557306	2.149861	0.408828	0	1.333451	0.889024	0.435124
0.2	2.479933	2.013727	0.641431	1	2.557306	2.149861	0.408828
0.3	2.323958	1.812462	0.44671	5	5.857327	6.559941	0.527087
m	Gr = Gc = 0, β = 0, $K = 0.1$, $S = 2.15$, $R = 1$			Pr	Gr = Gc = 0, β = 0, $k = 0.1$, $m = 0.5$, $R = 1$, $S = 2.15$		
0	2.448869	–0.08894	0.388587	0.7	2.398816	2.063803	0.450311
0.5	2.557306	2.149861	0.408828	1.0	2.557306	2.149861	0.408828
1.0	2.677826	4.627294	0.44507	1.5	0.83723	1.741461	0.009823
R	Gr = Gc = 0, β = 0, $k = 0.1$, $m = 0.5$, $S = 2.15$			β	Gr = Gc = 0, β = 0, $k = 0.1$, $m = 0.5$, $S = 2.15$		
1	2.557306	2.149861	0.408828	0	2.787661	2.426338	0.851939
4	2.476165	2.054473	0.791941	4	5.93695	6.435586	–7.633

the point of inflexion in all the profiles is observed at η = 1.2. It is also seen that the angular velocity decreases with increase in β, whereas the reverse effect occurs with increase in Gr.

The temperature profiles for different values of S, Δ, Gr, and β both in the absence and in the presence of solutal buoyancy are presented in Figs. 7 and 8, respectively. From Fig. 7 it is seen that the fluid temperature decreases with increase

in the heat source parameter. The temperature is seen to decrease with increase in S. The peculiarity of the present results is that the presence of thermal buoyancy decreases the temperature at all points in the thermal boundary layer in the absence of a source ($\beta = 0$). Figure 8 shows the temperature profiles for different values of the material parameter Δ in the presence of solutal buoyancy. It is found that the fluid temperature increases with Δ.

The effects of the Schmidt number and the chemical reaction parameter on the concentration profile were also considered. It was shown that the presence of a heavier species and an increase in the chemical reaction parameter decrease the concentration, so that the solutal boundary layer becomes thinner.

Finally, the numerical calculations for obtaining the local skin friction coefficient $f''(0)$, couple stress coefficient $h'(0)$, and the local Nusselt number, i.e., the wall temperature gradient $\theta'(0)$, were performed. The results presented in Table 1 are found to be in good agreement with those from [24]. It is seen from the table that the skin friction, couple stress, and the Nusselt number increase with the suction parameter in the absence of thermal buoyancyand a heat source, whereas the reverse effect occurs in their presence. The increase in the material parameter decreases all the characteristics. It is also seen that an increase in the Prandtl number in the absence of thermal buoyancy and a heat source increases the skin friction and couple stress for lower value of Pr, but further they decrease. The influence of radiation and the heat source presence on the characteristics mentioned was also considered.

Thus, the dependences of the profiles of the velocity, angular velocity, and the temperature, as well as of the values of the skin friction, couple stress, and the Nusselt number, on the problem parameters, have been obtained.

NOTATION

c, shrinking constant; c_p, specific heat; C, concentration; D, mass diffusivity; f, dimensionless stream function; Gr, thermal Grashof number; Gc, solutal Grashof number; g, acceleration due to gravity; h, dimensionless angular velocity; j, microinertia per unit mass; k, absorption coefficient; Kc^*, chemical reaction parameter; N, microrotation (angular) velocity; Pr, Prandtl number; Q^*, heat generation/absorption parameter; q_r, radiative heat flux; R, thermal radiation parameter; S, wall mass transfer parameter; Sc, Schmidt number; T, temperature; u, velocity component in the x direction; U_w, wall velocity; v, velocity component in the y direction; v_w, suction (injection) velocity; x, coordinate along the sheet; y, normal coordinate; β, heat source parameter; β' and β^*, volumetric coefficients of thermal and concentration expansion; γ, spin gradient viscosity; Δ, material parameter; η, similarity variable; θ, dimensionless temperature; κ vortex viscosity (gyroviscosity); κ^*, thermal conductivity of the fluid; μ, dynamic viscosity; ρ, fluid density; σ, Stefan–Boltzmann constant; υ, kinematic viscosity; Ψ, stream function. Indices: w, at the wall; ∞, in the free stream.

REFERENCES

1. A. C. Eringen, Theory of micropolar fluids, *J. Math. Mech*., **16**, 1–18 (1966).
2. G. Ahmadi, Self-similar solution of incompressible micropolar boundary layer flow over a semi-infinite plate, *Int. J. Eng. Sci*., **14**, 639–646 (1976).
3. R. S. R. Gorla, Micropolar boundary layer flow at a stagnation on a moving wall, *Int. J. Eng. Sci*., **21**, 25–33 (1983).
4. L. J. Crane, Flow past a stretching plate, *Z. Angew. Math. Phys.*, **21**, 645–647 (1970).
5. C. Y. Wang, Liquid film on an unsteady stretching sheet, *Q. Appl. Math*., **48**, 601–610 (1990).
6. T. Hayat and M. Qasim, Radiation and magnetic field effects on the unsteady mixed convection flow of a second grade fluid over a vertical stretching sheet, *Int. J. Numer. Methods Fluids*, **66**, 820–832 (2011).
7. D. Pal and H. Mondal, MHD non-Darcy mixed convective diffusion of species over a stretching sheet embedded in a porous medium with non-uniform heat source/sink, variable viscosity and Soret effect, *Commun. Nonlinear Sci. Numer. Simul*., **17**, 672–684 (2012).
8. R. Cortell, Analysing flow and heat transfer of a viscoelastc fluid over a semi-infinite horizontal moving flat plate, *Int. J. Non-Linear Mech*., **43**, 772–778 (2008).
9. K. Bhattacharya, Boundary layer stagnation-point flow of Casson fluid and heat transfer towards a shrinking/stretching sheet, *Front. Heat Mass Transf*., **4**, No. 023003, 1–9 (2013).
10. N. A. Yacob, A. Ishak, and I. Pop, Melting heat transfer in boundary layer stagnation point flow towards a stretching/shrinking sheet in a micropolar fluid, *Comput. Fluids*, **47**, 16–21 (2011).
11. M. Miklavčič and C. Y. Wang, Viscous flow due a shrinking sheet, *Q. Appl. Math.*, **64**, 283–290 (2006).

12. B. Mohanty, S. R. Mishra, and H. B. Pattnaik, Numerical investigation on heat and mass transfer effect of micropolar fluid over a stretching sheet, *Alexandria Eng. J*., **54**, No. 2, 223–232 (2015).
13. S. R. Mishra, G. C. Dash, and P. K. Pattnaik, Flow of heat and mass transfer on MHD free convection in a micropolar fluid with heat source, *Alexandria Eng. J*., **54**, No. 3, 681–689 (2015).
14. P. K. Rout, G. C. Dash, S. N. Sahoo, and S. R. Mishra, Chemical reaction effect on MHD free convection flow in a micropolar fluid, *Alexandria Eng. J*., **55**, No. 3, 2967–2973 (2016).
15. N. F. M. Noor, S. A. Kechil, and I. Hashim, Simple non-perturbative solution for MHD viscous flow due to a shrinking sheet, *Commun. Nonlinear Sci. Numer. Simul*., **15**, 144–148 (2010).
16. A. Ishak, Y. Y. Lok, and I. Pop, Stagnation-point flow over a shrinking sheet in a micropolar fluid, *Chem. Eng. Commun*., **197**, 1417–1427 (2010).
17. A. Ishak, Y. Y. Lok, and I. Pop, Non-Newtonian power-law fluid flow past a shrinking sheet with suction, *Chem. Eng. Commun*., **199**, 142–150 (2012).
18. S. Nadeem, Rizwan Ul Haq, and C. Lee, MHD flow of a Casson fluid over an exponentially shrinking sheet, *Sci. Iran. Trans. B: Mech. Eng. B*, **19**, No. 6, 1550–1553 (2012).
19. G. C. Dash, R. S. Tripathy, M. M. Rashidi, and S. R. Mishra, Numerical approach to boundary layer stagnation-point flow past a stretching/shrinking sheet, *J. Mol. Liquids*, **221**, 860–866 (2016).
20. T. Fang, S. Yao, J. Zhang, and A. Aziz, Viscous flow over a shrinking sheet with a second order slip flow model, *Commun. Nonlinear Sci. Numer. Simul*., **15**, 1831–1842 (2010).
21. C. Y. Wang, Stagnation flow towards a shrinking sheet, *Int. J. Non-Linear Mech*., **43**, 377–382 (2008).
22. T. Fang, J. Zhang, and S. Yao, Viscous flow over an unsteady shrinking sheet with mass transfer, *Chin. Phys. Lett.*, **26**, No. 1, 014703 (2009).
23. T. R. Mahapatra, S. K. Nandy, and A. S. Gupta, Momentum and heat transfer in MHD stagnation-point flow over a shrinking sheet, *ASME J. Appl. Mech*., **78**, 021015 (2011).
24. K. Bhattacharyya, S. Mukhopadhyay, G. C. Layek, and I. Pop, Effects of thermal radiation on micropolar fluid flow and heat transfer over a porous shrinking sheet, *Int. J. Heat Mass Transf*., **55**, 2945–2952 (2012).